

## Selective photoinduced antibacterial activity of amoxicillin coated gold nanoparticles. From one-step synthesis to *in vivo* cytocompatibility

M. Jazmín Silvero C., Diamela M. Rocca, Emilce Artur de la Villarmois; Kelsey Fournier; Anabel E. Lanterna; Mariela F. Pérez; M. Cecilia Becerra\* and Juan C. Scaiano\*

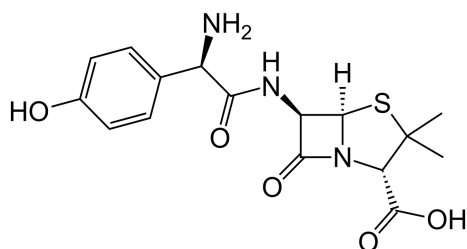


Figure S1. Amoxicillin molecular structure.

### Synthesis and Characterization of amoxi@AuNPs

The pale yellow solution of H<sub>2</sub>AuCl<sub>4</sub> turned slowly to red-violet after the addition of amoxicillin and heating to 50°C indicating the formation of AuNPs.<sup>1</sup> Final acidic solution (pH = 4.0) is generated by the dissociation of H<sub>2</sub>AuCl<sub>4</sub> to release H<sup>+</sup> ions, which in turn allows electrostatic interactions between the amoxicillin amine group (pK<sub>a</sub> = 7.5) and AuCl<sub>4</sub><sup>-</sup> ions. After washing three times no more amoxicillin was detected by UV-spectroscopy in the supernatant, and the pH was between 6.5 and 7.0, in agreement with that for ultrapure water. Transmission electron micrographs revealed different amoxi@AuNPs shapes and sizes (Figure S2). The majority of the population is composed by nano-spheres and nano-dodecahedrons (from 35 to 55 nm); however, triangular and hexagonal micro-plates (50 to 90 nm) and a few nanorods (Figure S3) could be observed. The nanoplates would most likely be the result of the slow reduction of some gold ions. We anticipate that amoxicillin will absorb rapidly on AuNP due to covalent interactions with their surface.<sup>2-3</sup> Overall, the statistical shape and size analysis performed with ImageJ (Figure S4) indicated that 86 % of the nanoparticles are spherical (average 50 nm) as displayed on the graph in Figure S2.

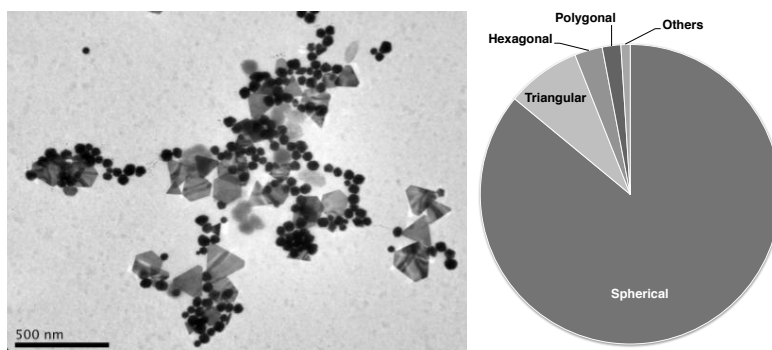


Figure S2. Amoxi@AuNP TEM picture (left) and its composition plot (right). The nanostructure solution is composed by 86 % spheres (average diameter:  $50 \pm 2$  nm), 8 % of triangular nanoplates (average side:  $100 \pm 13$  nm), 3 % of hexagonal nanoplates (average side:  $77 \pm 7$  nm), 2 % of irregular polygonal nanoplates and 1 % of other shapes including nanorods (length < 100 nm).

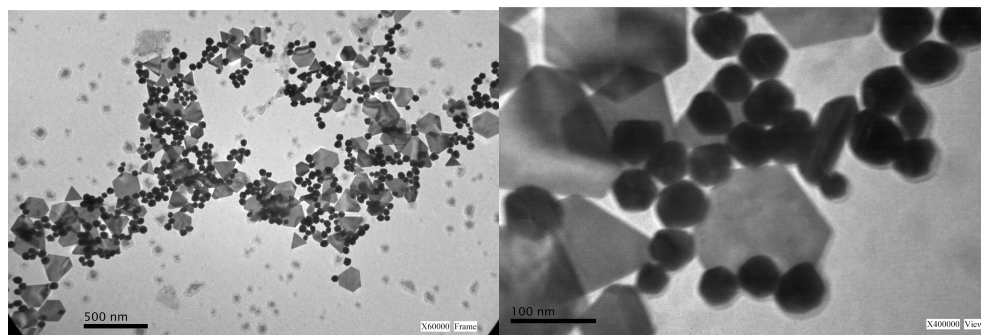


Figure S3. Additional TEM pictures of amoxi@AuNP.

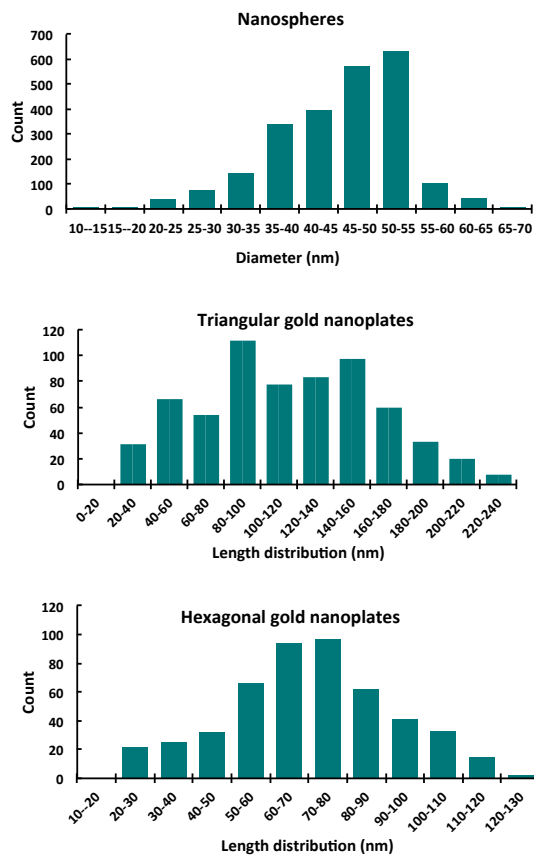


Figure S4. Size distribution of gold nanospheres (n=2353), triangular (n=642) and hexagonal gold nanoplates (n=489).

Characteristic bands of amoxicillin<sup>4</sup> (3459 cm<sup>-1</sup>, N-H stretching; 1687 cm<sup>-1</sup>, C=O stretch of the primary amine; 1771, C=O stretch of the  $\beta$ -lactam ring) were found in the FT-IR spectrum of the antibiotic alone (Figure S5a). As expected, these signals shifted to higher frequencies in the FT-IR spectra of the amoxi@AuNP sample, pointing to the successful binding of the amoxicillin molecule to the nanoparticle.<sup>5-8</sup> It is noteworthy that the active site of the antibiotic is preserved through the conjugation with the nanoparticle surface, since the signal of the C=O stretch of the  $\beta$ -lactam ring remains in the FT-IR spectrum of amoxi@AuNPs.

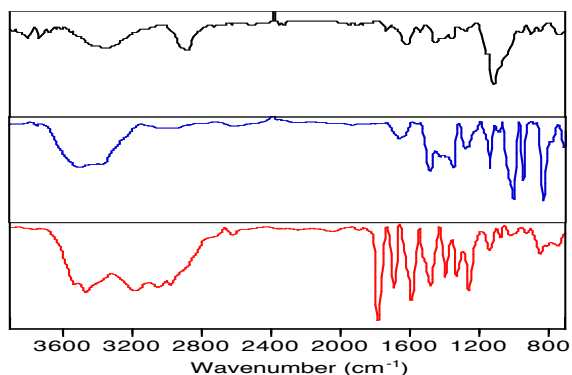


Figure S5. FT-IR spectrum of pure amoxicillin (red); AuNPs synthesized using NaBH<sub>4</sub> (blue); and AuNPs synthesized using amoxicillin (black). See experimental section for further details.

## Stability of amoxi@AuNPs in biological media

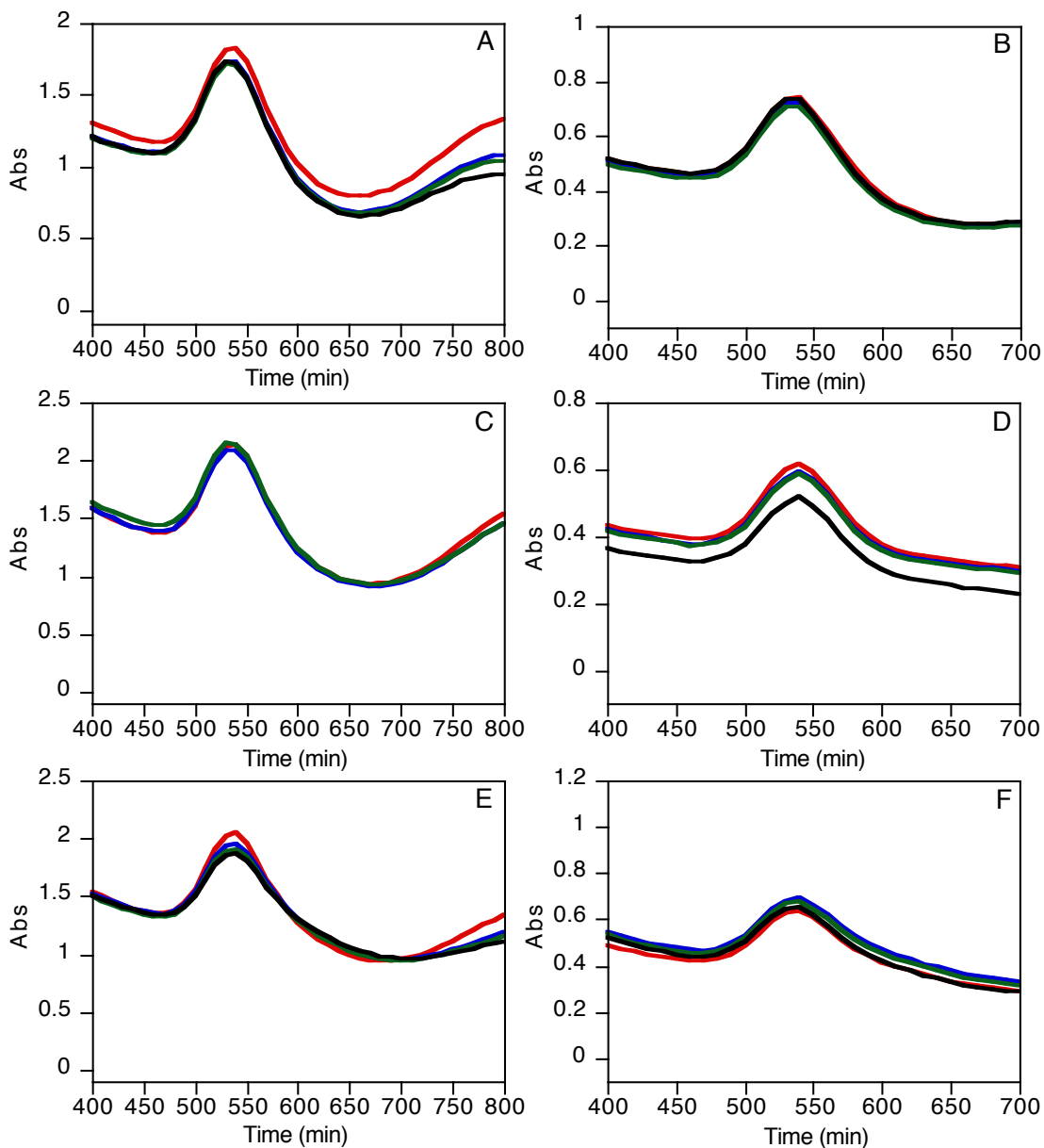


Figure S6. Absorption spectra of amoxi@AuNP showing stability versus time in different aqueous media: PBS 25.0 % (A), PBS 37.5% (B), Tryptic Soy Broth 25.0% (C), Luria Bertani Broth 12.5% (D), Mueller Hinton Broth 25.0% (E), Brain-Heart Broth 25.0% (F).



Figure S7. B/W images of LED panel (23.5 x 16.5 cm) used to irradiate well-plates. Irradiance ( $W/m^2$ ): red 55, red 99, blue 22, composed white 31.

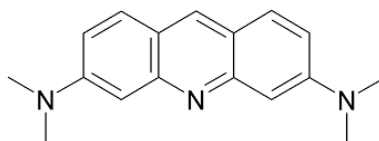


Figure S8. Acridine orange molecular structure.

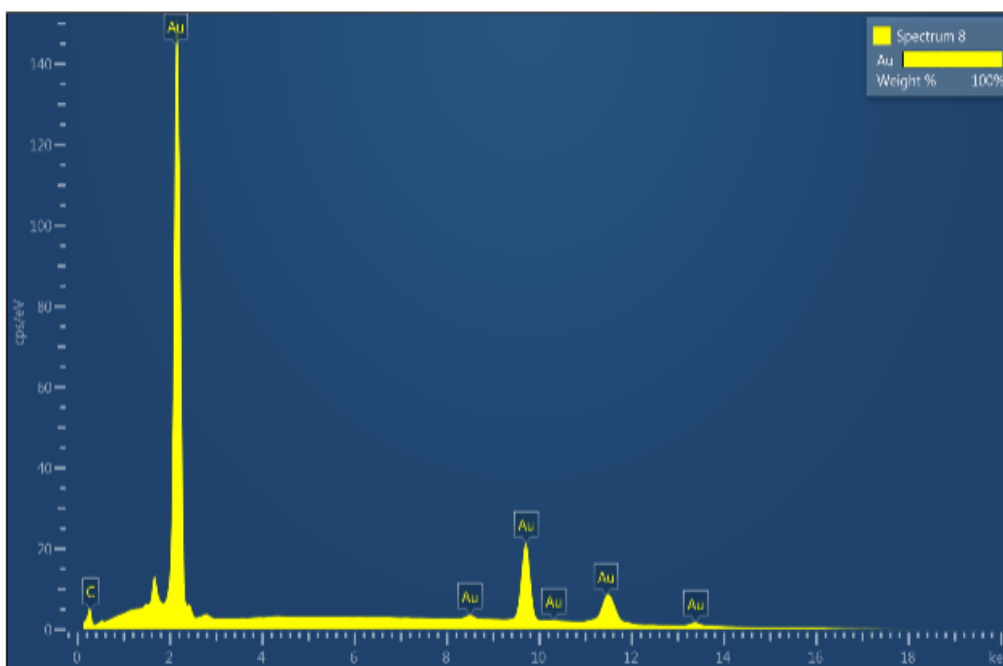


Figure S9. EDS on gold nanoplates synthesized with amoxicillin.

## References

1. Uppal, M. A.; Kafizas, A.; Ewing, M. B.; Parkin, I. P., The room temperature formation of gold nanoparticles from the reaction of cyclohexanone and auric acid; a transition from dendritic particles to compact shapes and nanoplates. *J. Mater. Chem. A* **2013**, *1* (25), 7351-7359.
2. Sainsbury, T.; Ikuno, T.; Okawa, D.; Pacile, D.; Frechet, J. M. J.; Zettl, A., Self-assembly of gold nanoparticles at the surface of amine- and thiol-functionalized boron nitride nanotubes. *J. Phys. Chem. C* **2007**, *111* (35), 12992-12999.
3. Bakshi, M. S.; Kaur, H.; Khullar, P.; Banipal, T. S.; Kaur, G.; Singh, N., Protein Films of Bovine Serum Albumen Conjugated Gold Nanoparticles: A Synthetic Route from Bioconjugated Nanoparticles to Biodegradable Protein Films. *J. Phys. Chem. C* **2011**, *115* (7), 2982-2992.
4. Bisson-Boutelliez, C.; Fontanay, S.; Finance, C.; Kedzierewicz, F., Preparation and Physicochemical Characterization of Amoxicillin beta-cyclodextrin Complexes. *AAPS PharmSciTech* **2010**, *11* (2), 574-581.
5. Rastogi, L.; Kora, A. J.; Arunachalam, J., Highly stable, protein capped gold nanoparticles as effective drug delivery vehicles for amino-glycosidic antibiotics. *Mater. Sci. Eng. C Mater. Biol. Appl.* **2012**, *32* (6), 1571-1577.
6. Sofokleous, P.; Stride, E.; Edirisinghe, M., Preparation, Characterization, and Release of Amoxicillin from Electrospun Fibrous Wound Dressing Patches. *Pharm. Res.* **2013**, *30* (7), 1926-1938.
7. Crespilho, F. N.; Lima, F. C. A.; da Silva, A. B. F.; Oliveira, O. N.; Zucolotto, V., The origin of the molecular interaction between amino acids and gold nanoparticles: A theoretical and experimental investigation. *Chem. Phys. Lett.* **2009**, *469* (1-3), 186-190.
8. Leff, D. V.; Brandt, L.; Heath, J. R., Synthesis and characterization of hydrophobic, organically-soluble gold nanocrystals functionalized with primary amines. *Langmuir* **1996**, *12* (20), 4723-4730.